Korean J. Chem. Eng., 35(4), 867-874 (2018)
DOI: 10.1007/s11814-017-0345-1

pISSN: 0256-1115
eISSN: 1975-7220

Methanol aromatization over CrZn-modified HZSM-5 catalysts

Bei Liu*, Siwu Lu*, Enzhou Liu*, Xiaoyun Hu, and Jun Fan*,†**

*School of Chemical Engineering, Northwest University, Xi'an 710069, P. R. China
**School of Physics, Northwest University, Xi'an 710069, P. R. China
(*Received 20 September 2017 • accepted 12 December 2017*)

Abstract−HZSM-5 (HZ) zeolite co-modified with Zn and second promoters (Zr, Ce, Mo and Cr) was synthesized and the aromatization of methanol over the modified HZ in a fixed-bed reactor was investigated. The results of catalytic tests revealed that the methanol conversion and yield of benzene, toluene, and xylene (BTX) over the Cr, Zn co-modification HZ (CrZn/HZ) were higher than that over ZrZn/HZ, CeZn/HZ, and MoZn/HZ. The catalysts were characterized by XRD, SEM, TEM, XPS, N_2 isothermal adsorption-desorption and NH_3-TPD. The results suggest that Zn species exist in two forms in the HZ zeolite. One is ZnO particle, the other one is $ZnOH^+$, which significantly improveds the yield of BTX. Furthermore, the Cr species on the external surface promoted the dispersion of ZnO, increased the amount of $ZnOH^+$, which further improved the yield of BTX. In addition, the optimal Cr_2Zn_1/HZ catalyst exhibited better catalytic performance and prolonged lifetime of reaction.

Keywords: Methanol to Aromatics, Bimetal-modified, CrZn/HZSM-5, BTX, $ZnOH^+$

INTRODUCTION

Aromatics, especially benzene, toluene and xylene (BTX), are widely employed as most important fundamental intermediates in the production of petrochemicals, medicine, cosmetics and pigments etc. BTX products originate from catalytic-reforming processes of naphtha or light paraffins refined from petroleum [1,2]. Recently, with the gradual depletion of oil resources and the rapid rise of demand for aromatics, alternative technology in non-traditional way has become quite necessary even though the oil price shows a downward trend [3,4]. The methanol to aromatics (MTA) process on microporous solid acid catalysts has increasingly attracted attention since Exxon Mobil first developed the ZSM-5 zeolite as catalyst for the methanol to gasoline (MTG) process in the 1970s. The industrialization of MTA is considered a potential route for utilizing the excessive coal-based methanol and meeting the market demand of BTX [5].

HZSM-5 (HZ) zeolite has been confirmed as an excellent aromatization catalyst because of its suitable acidic properties and three-dimensional, ordered, 10-ring pore corresponding with BTX molecules [6]. Many studies have reported that the incorporation of metal species over HZ zeolites could optimize the performance of methanol aromatization. Inoue et al. [7] found that the addition of Ag^+ ions into HZ catalyst obviously increased the selectivity for aromatic hydrocarbons in the conversion of methanol. However, the catalysts rapidly deactivated because of Ag^+ ions easily turning into Ag metal in the reductive atmosphere. H-GaMFI with isomorphous substitution and Ga/HZ with formic acid impregnation have been used for methanol-to-aromatics and propane aromatization, respectively. The Ga species greatly improved the aromatization performance, but the yield of light aromatic and the life span were unsatisfactory in the catalyst evaluation [8]. Compared with Ag, Ga, Mo metals, Zn species modified HZ presented excellent initial selectivity of BTX. Ni et al. [9] reported that the H[Zn, Al]ZSM-5 zeolite has a long life span of more than 160 h. However, the BTX yield is lower than 48%. Zhang et al. [10] confirmed that the high BTX yield of 67.7% was obtained on the Zn/HZ catalyst under the optimized conditions, which was due to its suitable distribution of acid sites as well as the small crystal size in favor of molecule diffusion. Although these catalysts exhibited superior yield of BTX, the poor stability of mono-metal modified HZ caused by rapid coke deposition and the loss of the active site limited their applications. To acquire efficient and stable modified catalyst, more attention was paid to the cooperation multi-element with HZ to improve the catalytic performance. The effect of La and P addition on the physicochemical properties and catalytic performances of Zn/HZ in FCC gasoline upgrading were investigated by Long et al. [11]. The synergistic effect of La and P increased the amount of $ZnOH^+$ species while preventing the loss of zinc species, which increased the activity for FCC gasoline aromatization and the stability of the catalyst. Xin et al. [12] found that a bimetal-modified Zn-Sn/HZ zeolite greatly improved the BTX yield to 64.1%, which was much higher than that attained on other mono-metal modified HZ catalysts such as Zn/HZ and Sn/HZ, but the catalyst Zn-Sn/HZ began to deactivate at 14 h and the methanol conversion dropped to about 20% after 17 h.

Many experts also applied the special features of transition metals to adjust the acid distribution of HZ for the enhancement of the catalytic ability. Majhi et al. [13] studied the direct conversion of methane mingled with the co-reactant methanol to higher hydrocarbons over the bimetal Zn-Mo/HZ. The optimum methane conversion could reach to 30.7% because of decreasing the activa-

†To whom correspondence should be addressed.
E-mail: fanjun@nwu.edu.cn

tion energy for the reaction by the synergy effect of the Zn and Mo species. Hadi et al. [14] introduced a second metal into the Mn/HZ, then attained higher selectivity of propylene in the process of methanol conversion to propylene (MTP) over the Ce modified Mn/HZ. Alyani et al. [15] prepared Fe loaded HZ to increase the yield of light olefins compared with unmodified HZ at the same operating conditions. Amin et al. [16] investigated the activity of Cr, Cu and Ga modified HZ for methane to liquid hydrocarbons. The amount of liquid hydrocarbons was obviously increased, because the strength of the Brønsted acid sites was weaken with the addition of Cr species. Mysov et al. [17] studied the conversion of synthesis gas into hydrocarbons over the ZnCr/ZSM-5 by physical mixing method.

In this study, we investigated the effect of Mo, Ce, Zr, Cr as the second promoters on the performance of Zn/HZ. The catalytic performance of M-Zn/HZ (M=Mo, Ce, Zr, Cr) was investigated, and the results suggested that CrZn/HZ exhibited higher methanol conversion and yield of BTX. XRD, TEM, SEM were applied to characterize the crystal structure and crystallinity, tissue, morphology. NH_3-TPD, N_2 absorption-desorption were employed to illustrate acid distribution, BET surface area and pore volume. TGA, XPS and catalytic performance were used to elucidate the process of MTA, life span of catalyst and anti-coking ability. The catalytic performance of the bimetal-modified catalysts was evaluated for the aromatization of methanol in a fixed-bed reactor to determine the relationship between the structure, acidic properties and catalytic properties of the zeolites.

EXPERIMENTAL

1. Catalyst Preparation

Incipient wetness impregnation was used to add the bi-metal into HZ zeolite. In a typical procedure, 3 g of HZ (SiO_2/Al_2O_3 mole ratio of 50, Nankai university) was added to 3 mL of a mixed aqueous solution containing zinc nitrate ($Zn(NO_3)_2{\cdot}6H_2O$, Chengdu Chem., A.R.) and the second nitrates ($Mo(NO_3)_3{\cdot}5H_2O$, Shanghai Chem., A.R.), ($Ce(NO_3)_3{\cdot}6H_2O$, Tianjin Chem., A.R.), ($Zr(NO_3)_4{\cdot}5H_2O$, Tianjin Chem., A.R.), ($Cr(NO_3)_3{\cdot}9H_2O$, Tianjin Chem., A.R.). The resulting mixture was stirred for 10 h at room temperature after ultrasonic treatment for 1 h, followed by drying at 110 °C overnight. Thereafter, the obtained precursor was calcined at 550 °C for 5 h under static air in a muffle oven to obtain the containing bimetal-modified HZ catalyst. The resultant solid was named as M_xZn_y/HZ, in which x and y expressed amount of the M and Zn loading, respectively, likely 1 wt% M and 1 wt% Zn modified HZ noted as M_1Zn_1/HZ. Then the calcined powder was pressed, crushed, sieved into 0.25-0.42 mm (40-60 mesh) particles prepared for the catalytic reaction.

2. Catalyst Characterization

The powder X-ray diffraction (XRD) of the synthesized zeolite samples was analyzed on Shimadzu XRD-6000 powder diffractometer using Cu Kα radiation (λ=1.5406 Å). The patterns were obtained in the 2θ range of 5°-60° with 0.02° step size. The Brunauer-Emmett-Teller (BET) surface area and pore volume of the catalysts were measured in the N_2 adsorption desorption method on the Quantachrome NOVA 2000e sorption analyzer at 77.40 K. The morphology of the catalysts was determined by scanning electron microscopy (SEM) recorded on the JEOL JSM-6390A system. Transmission electron microscopy (TEM) images of the optimal catalyst and the HZ were taken with a Hitachi H-800 electron microscope. NH_3 temperature programmed desorption (NH_3-TPD) was performed to measure the acidic amounts of the zeolite on a Micromeritics Chemisorb 2720 instrument. Approximately 0.1 g sample was taken in a U-type quartz tube and then pretreated in helium at 400 °C for 1 h, cooled to 100 °C and adsorbed NH_3 for 30 min. After flushing by pure helium flow at 100 °C for 30 min, the catalyst was heated (10 °C/min) to 700 °C, and the signal was recorded with a thermal conductive detector (TCD). Thermogravimetric analysis (TGA) was used to quantify coke formation on the catalyst on a NETZSCH STA 449F3 thermogravimetric analyzer. The used catalysts were treated by raising the temperature to 800 °C at a rate of 10 °C/min in flowing air. X-ray photoelectron spectroscopy (XPS) measurements were obtained with a Kratos AXIS NOVA spectrometer with an Al Kα radiation source (hν=1486.6 eV). The binding energy (BE) values were calibrated with the signal of contaminated carbon C1s at 284.8 eV.

3. Catalytic Tests

The MTA reaction was performed in a continuous flow fixed-bed stainless steel reactor (340 mm length and 9 mm inner diameter). 1 g of the sieved zeolite catalyst (40-60 mesh) was loaded and pretreated in a 55 mL/min N_2 flow at 500 °C for 2 h. Then, methanol was pumped into the reactor with a liquid hourly space velocity (LHSV) of 1.2 h^{-1}, and was converted into hydrocarbon in a 25 mL/min N_2 flow at 430 °C, 0.1 Mpa.

The mixed stream was online analyzed by a gas chromatograph (FULI 9790II) equipped with a flame ionization detector (FID) and a capillary column (SE-54, 30 m×0.32 mm×0.33 μm). When the gaseous mixture passed through the circuit water cooler, the gas and liquid products were separated. The residual gas was analyzed by a gas chromatograph (Shimadzu GC-14C) fitted with a thermal conductivity detector (TCD) and a Porapak-Q column (3 m×3 mm×2 mm). The conversion of methanol and the yield of products were calculated from the number of carbon atoms in the calibration normalization method.

RESULTS AND DISCUSSION

1. Catalytic Tests of the $M_{0.5}Zn_1/HZ$ Catalysts

The catalytic performance of $M_{0.5}Zn_1/HZ$ (M=Ce, Mo, Zr, and Cr; 0.5 and 1 represent 0.5 wt% and 1.0 wt%, respectively) was investigated. The conversion of methanol, the yield of BTX and the distribution of hydrocarbons are presented in Fig. 1. As shown in Fig. 1(a), the conversion of methanol and the yield of BTX over $Cr_{0.5}Zn_1/HZ$ (100%, approx. 45%, respectively) were high and changed little with the reaction time, indicating that the $Cr_{0.5}Zn_1/HZ$ catalyst had high catalytic activity and stability. However, the conversion of methanol and the yield of BTX over other catalysts decreased rapidly, especially the $Zr_{0.5}Zn_1/HZ$ catalyst.

Fig. 1(b) displays the distribution of products over the different promoter modified HZ. The complex hydrocarbon products, such as C_1-C_2, C_3, C_4, C_5, C_5+ aliphatics, BTX (benzene, toluene, xylene), C_9 (trimethylbenzene) and C_9+ aromatics were obtained in the

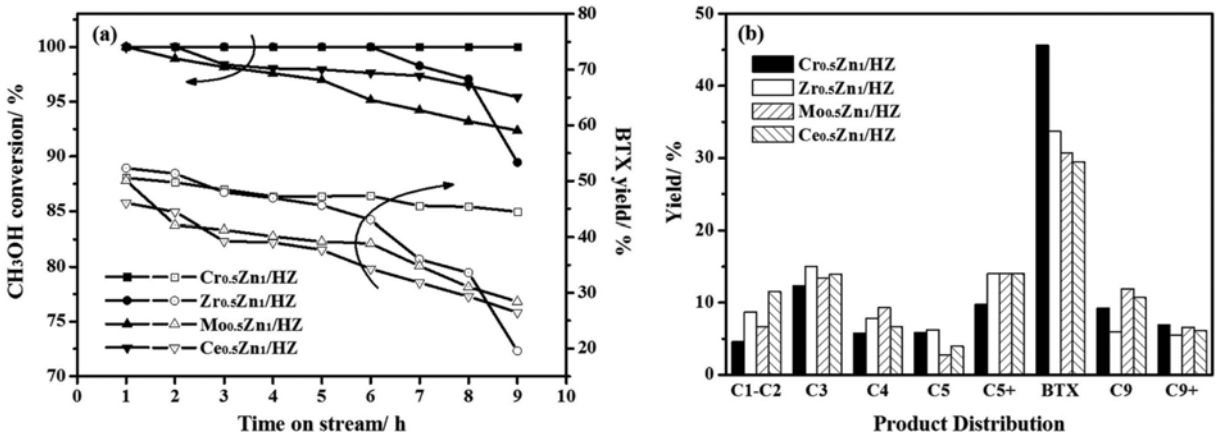

Fig. 1. (a) The conversion of methanol and the yield of BTX over the $M_{0.5}Zn_1$/HZ (M=Cr, Zr, Mo and Ce) catalysts. (b) The distribution of hydrocarbons over the $M_{0.5}Zn_1$/HZ (M=Cr, Zr, Mo and Ce) catalysts at the 8th hour. Reaction conditions: T=430 °C; LHSV=1.2 h^{-1}; the flow of N_2=25 mL/min; P=0.1 Mpa.

MTA reaction. It could be attributed to a series of reactions on the catalyst, which included dehydration, oligomerization, cracking, hydrogen transfer, dehydrocyclization, aromatization, etc [9,18]. Combined with Fig. 1(a), the methanol conversion of $Cr_{0.5}Zn_1$/HZ maintained 100%, while those of $Zr_{0.5}Zn_1$/HZ, $Ce_{0.5}Zn_1$/HZ, $Mo_{0.5}Zn_1$/HZ dropped to 96.84%, 96.29%, 92.93% after 8 h on stream, respectively. Meanwhile, the $Cr_{0.5}Zn_1$/HZ catalyst showed the highest yield of BTX production (45.58%) and the low yield of C_1-C_5 aliphatics (Fig. 1(b)), which was due to their strong aromatization ability that could convert the C_2, C_3, C_4 alkenes into aromatics [19]. In addition, compared with the $Cr_{0.5}Zn_1$/HZ catalyst, $Zr_{0.5}Zn_1$/HZ, $Ce_{0.5}Zn_1$/HZ and $Mo_{0.5}Zn_1$/HZ presented lower total yield of the hydrocarbons especially for the BTX yield.

Accordingly, $Cr_{0.5}Zn_1$/HZ catalyst was favorable for formation of aromatics with the higher methanol conversion while $Zr_{0.5}Zn_1$/HZ, $Ce_{0.5}Zn_1$/HZ, $Mo_{0.5}Zn_1$/HZ did not significantly improve the catalytic performance. $Cr_{0.5}Zn_1$/HZ catalyst was selected to investigate relationship of the structure and activity. Furthermore the appropriate concentration and adequate strength of acid sites depended on the promoters, which were crucial role for the MTA reaction. Therefore, the optimal ratio of chromium and zinc was further studied by varying the content of chromium.

2. Catalytic Tests of the Cr_xZn_1/HZ Catalysts

A series of activity tests were carried out using various catalysts with different loading of Cr and Zn species in the MTA reaction. In the stable process (during the first 8 hours), all catalysts represented high conversion of methanol, which reached to 100%. The yield of the production is depicted in Fig. 2. It is clear that the non-modified HZ catalyst exhibited only 32.44% yield of BTX with more than 55.40% yield of C_1-C_5+ hydrocarbons and 5.76% yield of C_9+ aromatics. When the Zn was introduced into the HZ zeolite, a large increment of the BTX yield was obtained at the expense of C_3, C_4 and C_5 hydrocarbons over the Zn_1/HZ catalyst. The result is consistent with a previous report that the zinc cations could act as catalysts for the dehydrogenation of alkanes, the light olefins formed can be dehydrogenated to aromatics over the zinc cations [20]. As shown in Fig. 2, the Cr, Zn co-impregnated

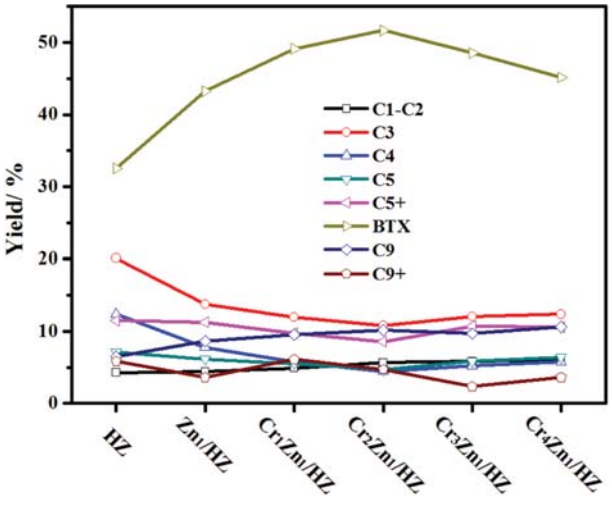

Fig. 2. The yield of hydrocarbons over the Cr_xZn_1/HZ catalysts with different Cr content for the MTA reaction. Reaction conditions: T=430 °C; LHSV=1.2 h^{-1}; the flow of N_2=25 mL/min; P=0.1 Mpa; time on stream (TOS)=8 h.

catalyst obviously showed higher yield of BTX than the catalyst modified by Zn only. The rising Cr loading brought about promoting the formation of the aromatics, whereas the excessive of Cr loading resulted in the decrement of the BTX and regained the high yield of C_3, C_4, C_5 hydrocarbons. Then the Cr_2Zn_1/HZ catalyst was considered as the optimum catalyst in the MTA reaction, which showed 51.70% BTX yield and low yield of C_1-C_5 hydrocarbons.

Generally, the formation of coke on catalyst surfaces causes catalyst deactivation over the MTA reaction [21]. To analyze the anti-coking performance and the catalytic stability, the TGA and DTG curves of the catalysts with different Cr content were measured, and the peak area on the DTG curves was proportional to the weight loss on the TG curves. As shown in Fig. 3, there are two different weight loss steps in the curves. The former is due to the removal of absorbed water from 150 °C to 300 °C and the latter is attributed

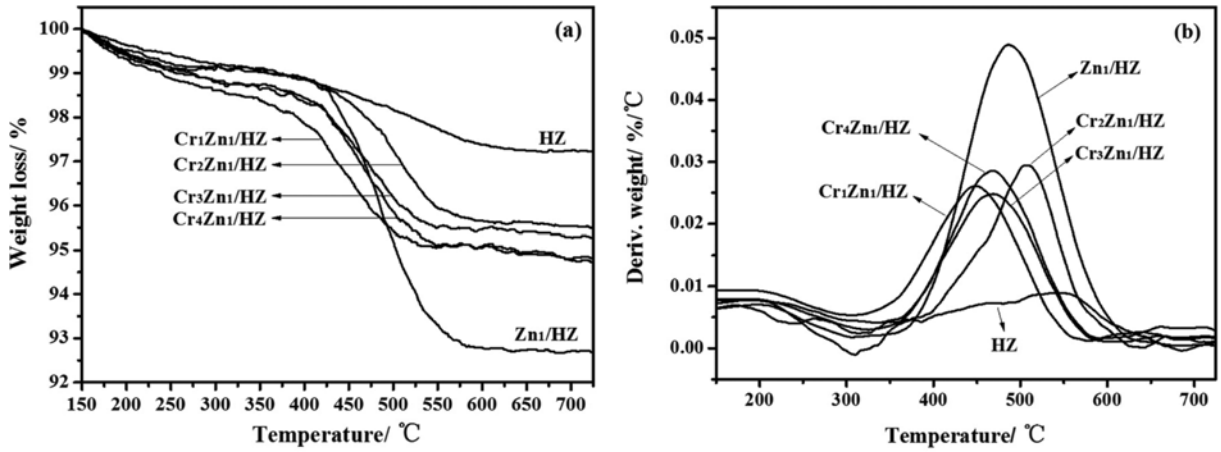

Fig. 3. TG (a) and DTG (b) curves of the Cr_xZn_1/HZ catalysts with different Cr content in aromatization for 8 h.

to the consumption of carbon deposited between 300 °C and 600 °C. Apparently, the weight loss of HZ (2.76%) was less than other modified catalysts, which was mainly induced by the weak aromatization performance and the formation of light aliphatics with low diffusion resistance. In contrast, Zn_1/HZ showed good dehydrogenation ability by the introduction of Zn species that improved the formation of big size intermediates [19], which led to the most serious coke deposition. As reported before, the impregnation of Cr in HZ might alleviate the formation of coke and promote the formation of aromatics [22]. Therefore, the weight loss of Cr_xZn_1/HZ catalysts was less than that of Zn_1/HZ. Moreover, with the increment of Cr loading, the content of coke was decreased from the Cr loading of 0% to 2% and increased after 2% (Fig. 3(a)). The results thus suggested that the Cr_2Zn_1/HZ had the lower mass of coke and exhibited better anti-coking ability. Additionally, it was speculated that the Cr_2Zn_1/HZ would displayed longer catalytic life span and more stable performance.

3. Catalyst Characterization

The X-ray diffraction (XRD) patterns of the modified catalysts are displayed in Fig. 4. All of the diffraction peaks agree with the typical MFI crystal structures, which demonstrates the lattice structure of HZ zeolite was still intact after Cr, Zn impregnation. Compared with the parent HZ, however, the intensity of the diffraction peaks of CrZn/HZ was decreased with the addition of the Cr and Zn species. This suggested that the CrZn/HZ had a lower crystallinity, which could be ascribed to the dispersion of the metals on the external surface or in the inner pore of the HZ zeolite [23]. Moreover, no diffraction peaks of ZnO in modified catalysts implied that Zn species were highly dispersed in the zeolites [9]. However, several peaks related to Cr_2O_3 (32.5° and 55°) were observed with

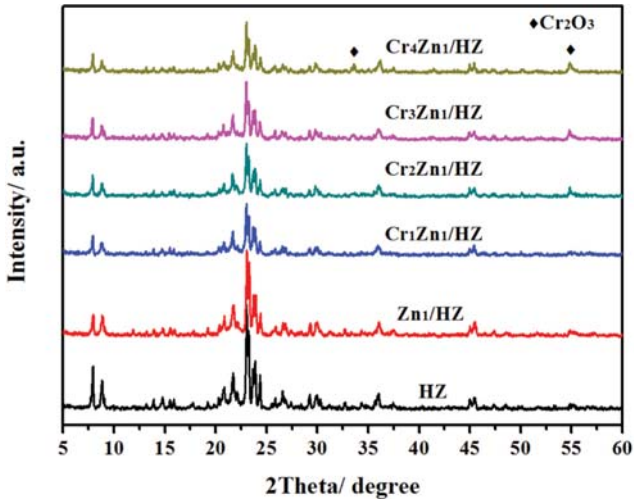

Fig. 4. XRD patterns of the Cr_xZn_1/HZ catalysts with different Cr content.

Table 1. Pore structure parameters of the Cr_xZn_1/HZ catalysts with different Cr content

Catalyst type	BET surface area ($m^2 \cdot g^{-1}$)	Micropore BET surface area[a] ($m^2 \cdot g^{-1}$)	Pore volume[b] ($cm^3 \cdot g^{-1}$)	Micropore volume[a] ($cm^3 \cdot g^{-1}$)
HZ	247	235	0.136	0.121
Zn_1/HZ	230	215	0.134	0.112
Cr_1Zn_1/HZ	223	207	0.131	0.107
Cr_2Zn_1/HZ	216	200	0.131	0.104
Cr_3Zn_1/HZ	214	196	0.130	0.102
Cr_4Zn_1/HZ	210	193	0.129	0.096

[a]t-Plot method
[b]Volume adsorbed at p/p_0=0.97

the increasing of Cr loading [16]. In the Cr_3Zn_1/HZ, Cr_4Zn_1/HZ catalysts, a fraction of the excessive amount of Cr loading self-assembled to form the bulk phase of Cr_2O_3, which might be independent of zeolite and made no contribution to the enhanced catalytic performance.

The texture properties of original HZ and various modified HZ are presented in Table 1. Based on results of N_2 adsorption desorption tests, with the introduction of Zn, Cr species into catalysts, the BET surface area and pore volume were lessened. It might be claimed that some pore channels were blocked or covered by the loading of Zn, Cr inside catalyst, which was in good agreement with the XRD results. Compared with the HZ, the Zn_1/HZ showed lower BET surface area and pore volume, so the micropore surface area and micropore volume were decreased. This suggests that various Zn species could coexist in the zeolite, such as the finely dispersed ZnO, $ZnOH^+$ inside the zeolite pore [24] and the ZnO particles on the external surface. Furthermore, the BET surface area and pore volume were decreased slightly in the Zn, Cr co-impregnated catalysts with the increment of Cr loading, indicating that the addition of Cr did not clog the pore channels and had a mild impact on the HZ catalyst.

Fig. 5 depicts SEM graphs of parent HZ, Cr_2Zn_1/HZ and TEM images of Cr_2Zn_1/HZ. In Fig. 5(a), the morphology of HZ is a typical hexagonal-shaped MFI crystal structure about 8 μm in length [24]. Meanwhile, the SEM micrographs of the Cr_2Zn_1/HZ zeolite show typical MFI structure as well as HZ morphology, which indicates that the addition of Cr, Zn had little influence on the morphology of HZ (Fig. 5(b)). As can been seen in the TEM images (Fig. 5(c), (d)), the ZnO and Cr_2O_3 particles ranging from 5-10 nm were represented by the dark spots and highly dispersed on the external surface of zeolite crystals. In addition, the presence of

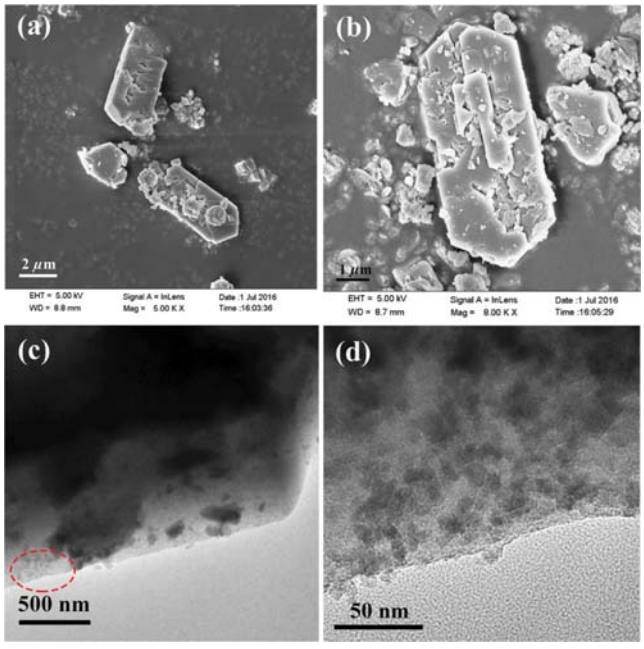

Fig. 5. The SEM photographs of (a) HZ and (b) Cr_2Zn_1/HZ. The TEM image of Cr_2Zn_1/HZ under different magnifications (c) 500 nm, (d) 50 nm.

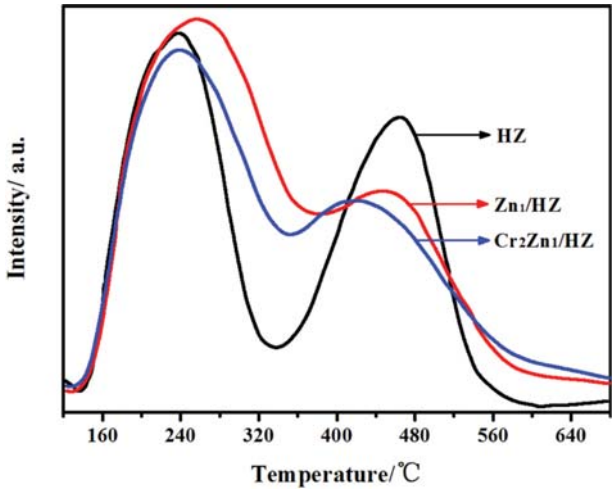

Fig. 6. NH_3-TPD profiles of HZ, Zn_1/HZ and Cr_2Zn_1/HZ catalysts.

the ZnO and Cr_2O_3 particles were also confirmed by XPS spectra in Fig. 7. Highly dispersed ZnO and Cr_2O_3 small particles could promote the formation of $ZnOH^+$ active center, which provided the opportunity for the methanol molecules to contact with the active center. In addition, the active centers were also conducive to the aromatization of lower alkenes by dehydrogenation, oligomerization and cyclization [11].

The strengths and the amounts of acid sites on the catalyst surface were measured by the NH_3-TPD, due to the absorption between the acid sites of catalysts and basic nature of ammonia. Fig. 6 shows the distribution and amounts of the acid sites in the HZ, Zn_1/HZ and Cr_2Zn_1/HZ catalysts. Generally, all samples exhibited two well ammonia desorption peaks, the high-temperature peak and the low-temperature peak, located at 450 °C and 230 °C, respectively [25,26]. The former was assigned to the high- and medium-strength acid site and the latter was assigned to the weak acid and metallic oxide. Compared with the original HZ, the low-temperature peak intensity was increased, but the intensity of the high-temperature peak was reduced in the Zn_1/HZ catalyst. Meanwhile, the high-temperature peak was shifted to lower temperature. The phenomenon might be attributed to the $ZnOH^+$ from the interaction between the zinc species and the internal/terminal silanol Si-OH or the bridging Si-OH-Al groups in the present HZ [27,28]. In the result, $ZnOH^+$ and the silanol groups or the bridging Si-OH-Al corresponded to the medium-strength acid and high-strength acid, respectively [27]. Therefore, the high-temperature peak of Zn_1/HZ was shifted to lower temperature compared with HZ. With the impregnation of Cr, the amount of acid sites was slightly decreased. Additionally, the high-temperature peak moved to the 400 °C. It seems that Cr loading promoted the dispersion of ZnO and increased the concentration of $ZnOH^+$ which was also confirmed by XPS spectra in Fig. 7. Many experts [27,29] confirmed that the $ZnOH^+$ significantly improved the methanol aromatization and suppressed the formation of light olefins. Consequently, it was consistent with the catalytic results in Fig. 2 that the modified catalysts displayed better selectivity of BTX.

The chemical states of the surface Zn, Cr species in the Cr_2Zn_1/

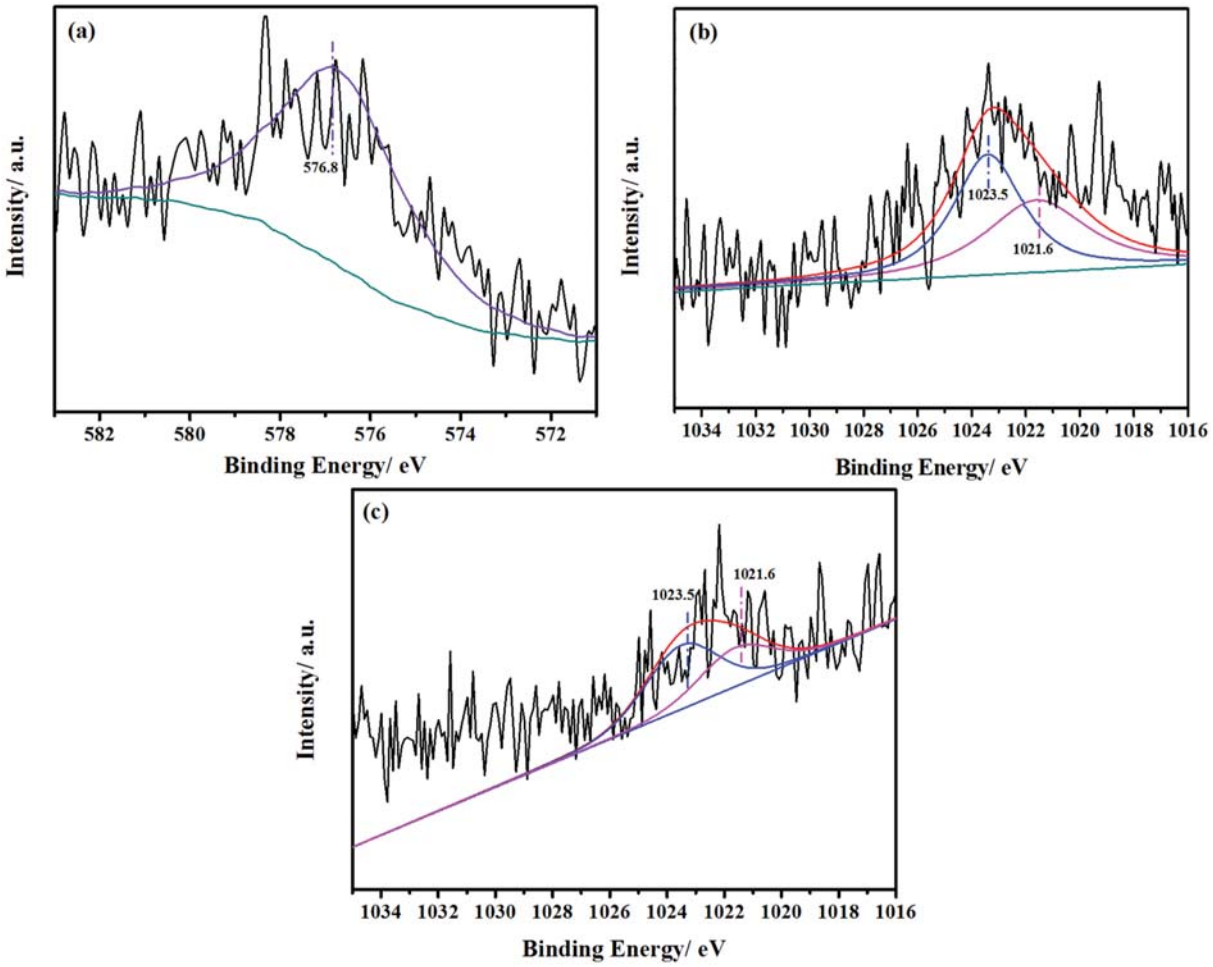

Fig. 7. XPS spectra of (a) Cr (2p3/2), (b) Zn (2p3/2) of the Cr_2Zn_1/HZ catalyst and (c) Zn (2p3/2) of the Zn_1/HZ catalyst.

HZ and Zn_1/HZ zeolite were characterized by XPS. As shown in Fig. 7(a), the Cr 2p3/2 XPS plectrum at 576.8 eV could be attributed to the Cr_2O_3 phase [30], which suggests that a portion of clusters loaded in the surface of Cr_2Zn_1/HZ was Cr_2O_3 species. The XPS spectra of Zn 2p3/2 were observed at binding energy 1,020-1,024 eV in Fig. 7(b) and (c). The convoluting of the Zn 2p3/2 XPS spectra discriminated two types of Zn species with binding energies around 1,023.4 eV and 1,021.6 eV. The lower binding energy at 1,021.6 eV indicated the ZnO clusters dispersed in the surface of zeolite [29,31], and the another binding energy at 1,023.4 eV was attributed to the $ZnOH^+$ species [27]. In Cr_2Zn_1/HZ, as shown in Fig. 7(b), the $ZnOH^+$ and ZnO species accounted for about 62% and 38%, respectively. And in Zn_1/HZ, as shown in Fig. 7(c), the $ZnOH^+$ and ZnO species were about 55% and 45%, respectively. In addition, the ZnO spectrum of Cr_2Zn_1/HZ was more broadened because of the high dispersion of ZnO species. Therefore, the Cr loading increased the concentration of $ZnOH^+$ and promoted the dispersion of ZnO species. The $ZnOH^+$ had about four nearest neighbor oxygen atoms without the next neighbor Zn and the ZnO clusters [28]. Also, it was formed from the tighter interaction between the zinc species and strong protonic acid sites which resulted in the decrement of strong acid according with the result in the NH_3-TPD.

4. Catalytic Stability Testing and Anti-coke Ability

In the industrialization process of the catalyst, the activity, stability and lifetime of catalyst were the main considerations. The con-

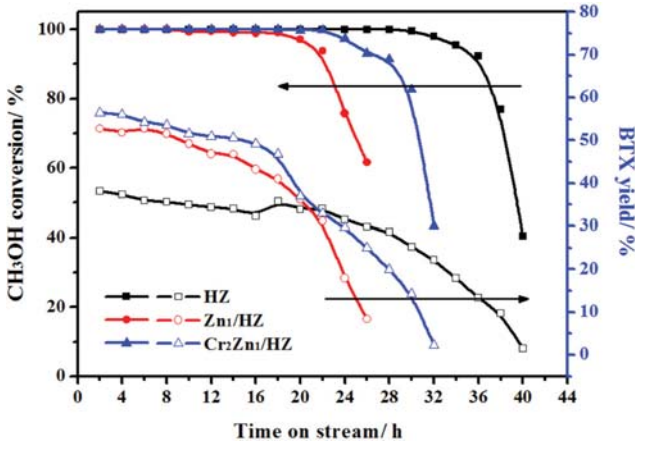

Fig. 8. Conversion of methanol and yield of BTX versus time on stream over HZ, Zn_1/HZ and Cr_2Zn_1HZ catalysts. Reaction conditions: T=430 °C; LHSV=1.2 h^{-1}; the flow of N_2=25 mL/min; P=0.1 Mpa.

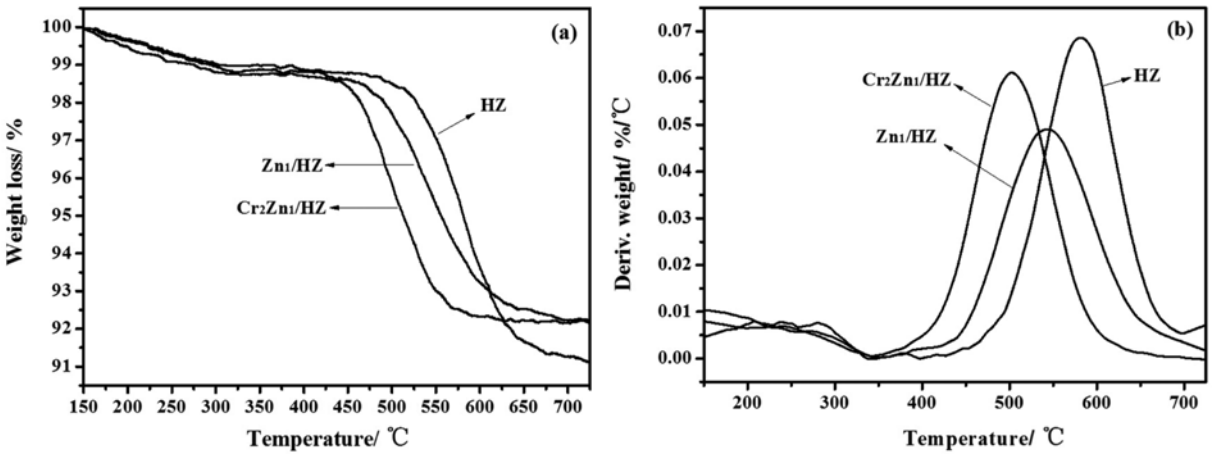

Fig. 9. TG (a) and DTG (b) curves of the HZ, Zn_1/HZ and Cr_2Zn_1/HZ catalysts in aromatization after deactivation.

version of methanol and BTX yield over HZ, Zn_1/HZ and Cr_2Zn_1/HZ catalysts versus time on stream is illustrated in Fig. 8. The HZ samples exhibited relatively long lifetime and the conversion of methanol was maintained at 100% for 30 h after the initial reaction and decreased to 39.58% after 40 h on stream. However, the HZ showed poor yield of BTX on stream. The introduction of Zn into HZ significantly improved BTX yield in the initial process but shortened the reaction lifetime. The methanol conversion of Zn_1/HZ was sharply reduced to 61.21% from 20 h to 26 h. Compared with Zn_1/HZ, Cr_2Zn_1/HZ showed slightly higher yield of BTX and longer reaction lifetime. Probably because the impregnation of Cr promoted the formation of $ZnOH^+$ and the dispersion of ZnO and alleviated the coking reaction. The $ZnOH^+$ could enhance the dehydrogenation of alkanes and aromatization of alkenes to aromatics and suppress the formation of light alkanes. However, the ZnO species was inactive for MTA.

In general, catalyst deactivation during the MTA process directly influenced the activation and stability. Fig. 9 depicts the weight loss of three deactivated HZ (TOS=40 h), Zn_1/HZ (TOS=26 h), Cr_2Zn_1/HZ (TOS=32 h) catalysts. The non-modified HZ shows long lifetime meanwhile exhibiting larger coke capacity (8.89%). The modified Zn_1/HZ and Cr_2Zn_1/HZ displayed lower coke capacity than that of HZ, which resulted from the Zn, Cr species occupying the portion of catalyst pore and surface. It was also revealed that the lower coking rate of Cr_2Zn_1/HZ than Zn_1/HZ. Xin et al. [12] reported the introduced second metal Sn, La and Ce combined with the defective sites in the HZ zeolite, where the micropores of zeolite were easily blocked due to the coke deposit by large detained intermediates. However, the dispersed metal species transformed intermediates to the surface from active sites. Therefore, it speculated that the impregnation of Cr prolonged the lifetime of MTA reaction by the decrement of coking rate. Besides, the decomposition temperature for coke on Cr_2Zn_1/HZ was lower than that of Zn_1/HZ and HZ, which was in favor of its regeneration process.

The MTA process involved complicated steps and overlapped reactions, like dehydration, oligomerization, methylation, cracking, hydrogen transfer, dehydrogenation and cyclization. The aromatics- and olefins- based cycle mechanism was dominant for the MTA reaction over HZ than over SAPO-34 and HZSM-22 for the MTH reaction [32,33]. In the dual-cycle mechanism, ethylene/aromatics were mainly produced via the aromatics, and higher alkenes were probably formed to considerable extent from successive alkene methylization and cracking reaction via the olefins-based cycle [34,35]. The higher olefins experienced dehydro-cyclooligomerization and hydrogen transfer reactions to produce aromatics and alkanes, which might connect the two cycles together. In the HZ zeolite, Brønsted acid sites were crucial to the formation of olefins from methanol. According to the results of NH_3-TPD, XPS spectra, the introduction of zinc species led to decrease of Brønsted acid sites [24,36] and the lower yield of alkanes by weakening the hydrogen transfer reaction. Furthermore, the $ZnOH^+$ species promoted the dehydrogenation and cyclization of alkenes to aromatics with the strong dehydrogenation and aromatization ability. The impregnation of Cr species increased the amount of $ZnOH^+$ and raised the yield of BTX, which was agreement with the report that the improvement of aromatics was linearly related to the amount of $ZnOH^+$ species [27]. Additionally, Cr_2Zn_1/HZ exhibited low coking rate and well reaction stability.

CONCLUSION

HZ zeolite co-modified with Zn and second promoters (Zr, Ce, Mo and Cr) was synthesized and conversion of methanol to aromatics over the modified HZ in a fixed-bed reactor was investigated. The results suggested that CrZn/HZ exhibits higher methanol conversion and the yield of BTX than the ZrZn/HZ, CeZn/HZ, MoZn/HZ catalysts. The introduction of Zn generated the new $ZnOH^+$ active site and decreased the amount of olefins by the better dehydrogenation ability and aromatization performance. However, the Zn/HZ presented poor reaction stability from the rapid carbon deposition. The impregnation of Cr improved the yield of BTX due to the dispersion of $ZnOH^+$. In addition, the restriction of coking could be achieved, because the Cr species combined with the defective sites to suppress the formation of coke on the active sites. Therefore, the optimal Cr_2Zn_1/HZ catalyst manifested good catalytic performance in the MTA reaction, which shows potential

application prospect for the industrialization of the MTA process.

ACKNOWLEDGEMENT

This work was supported by the National Natural Science Foundation of China (Nos. 21476183, 51372201 and 21676213).

REFERENCES

1. X. Xu, E. Jiang, Y. Du and B. Li, *Renew. Energy*, **96**, 458 (2016).
2. S. Phatanasri, P. Praserthdam and A. Sripusitto, *Korean J. Chem. Eng.*, **17**, 409 (2000).
3. S. Tamiyakul, S. Anutamjarikun and S. Jongpatiwut, *Catal. Commun.*, **74**, 49 (2016).
4. Y. Bi, Y. Wang, X. Chen, Z. Yu and L. Xu, *Chin. J. Catal.*, **35**, 1740 (2014).
5. F. Wang, W. Xiao, L. Gao and G. Xiao, *Catal. Sci. Technol.*, **6**, 3074 (2016).
6. J. Li, C. Hu, K. Tong, H. Xiang, Z. Zhu and Z. Hu, *RSC Adv.*, **4**, 44377 (2014).
7. Y. Inoue, K. Nakashiro and Y. Ono, *Micropor. Mater.*, **4**, 379 (1995).
8. H. Xiao, J. Zhang, X. Wang, Q. Zhang, H. Xie, Y. Han and Y. Tan, *Catal. Sci. Technol.*, **5**, 4081 (2015).
9. Y. Ni, A. Sun, X. Wu, G. Hai, J. Hu, T. Li and G. Li, *Micropor. Mesopor. Mater.*, **143**, 435 (2011).
10. G. Q. Zhang, T. Bai, T. F. Chen, W. T. Fan and X. Zhang, *Ind. Eng. Chem. Res.*, **53**, 14932 (2014).
11. H. Long, F. Jin, G. Xiong and X. Wang, *Micropor. Mesopor. Mater.*, **198**, 29 (2014).
12. Y. Xin, P. Qi, X. Duan, H. Lin and Y. Yuan, *Catal. Lett.*, **143**, 798 (2013).
13. S. Majhi, P. Mohanty, A. K. Dalai and K. K. Pant, *Energy Technol.*, **1**, 157 (2013).
14. N. Hadi, A. Niaei, S. R. Nabavi, M. Navaei Shirazi and R. Alizadeh, *J. Ind. Eng. Chem.*, **29**, 52 (2015).
15. M. Alyani, J. Towfighi and S. M. Sadrameli, *Korean J. Chem. Eng.*, **28**, 1351 (2011).
16. N. A. S. Amin and D. D. Anggoro, *J. Nat. Gas. Chem.*, **12**, 123 (2003).
17. V. Mysov, S. Reshetnikov, V. Stepanov and K. Ione, *Chem. Eng. J.*, **107**, 63 (2005).
18. A. Lacarriere, F. Luck, D. Świerczyński, F. Fajula and V. Hulea, *Appl. Catal. A: Gen.*, **402**, 208 (2011).
19. H. Schulz, *Catal. Today*, **154**, 183 (2010).
20. Y. Ono, H. Adachi and Y. Senoda, *J. Chem. Soc. Faraday Trans.*, **84**, 1091 (1988).
21. C. Sun, Y. Yang, J. Du, F. Qin, Z. Liu, W. Shen, H. Xu and Y. Tang, *Chem. Commun.*, **48**, 5787 (2012).
22. Z. Hajjar, A. Khodadadi, Y. Mortazavi, S. Tayyebi and S. Soltanali, *Fuel*, **179**, 79 (2016).
23. S. M. T. Almutairi, B. Mezari, P. C. M. M. Magusin, E. A. Pidko and E. J. M. Hensen, *ACS Catal.*, **2**, 71 (2012).
24. M. Fattahi, R. M. Behbahani and T. Hamoule, *Fuel*, **181**, 248 (2016).
25. N. Katada, H. Igi, A. Jongho Kim and M. Niwa, *J. Phys. Chem. B*, **101**, 5969 (1997).
26. L. Rodríguez-González, F. Hermes, M. Bertmer, E. Rodríguez-Castellón, A. Jiménez-López and U. Simon, *Appl. Catal. A: Gen.*, **328**, 174 (2007).
27. X. Niu, J. Gao, Q. Miao, M. Dong, G. Wang, W. Fan, Z. Qin and J. Wang, *Micropor. Mesopor. Mater.*, **197**, 252 (2014).
28. J. A. Biscardi, G. D. Meitzner and E. Iglesia, *J. Catal.*, **179**, 192 (1998).
29. X. Wang, J. Zhang, T. Zhang, H. Xiao, F. Song, Y. Han and Y. Tan, *RSC Adv.*, **6**, 23428 (2016).
30. M. Roy, S. Ghosh and M. K. Naskar, *Mat. Chem. Phys.*, **159**, 101 (2015).
31. N. Sapawe, A. A. Jalil, S. Triwahyono, R. N. R. A. Sah, N. W. C. Jusoh, N. H. H. Hairom and J. Efendi, *Appl. Catal. A: Gen.*, **456**, 144 (2013).
32. P. Tian, Y. Wei, M. Ye and Z. Liu, *ACS Catal.*, **5**, 1922 (2015).
33. J. Li, Y. Wei, G. Liu, Y. Qi, P. Tian, B. Li, Y. He and Z. Liu, *Catal. Today*, **171**, 221 (2011).
34. M. Bjorgen, S. Svelle, F. Joensen, J. Nerlov, S. Kolboe, F. Bonino, L. Palumbo, S. Bordiga and U. Olsbye, *J. Catal.*, **249**, 195 (2007).
35. S. Ilias and A. Bhan, *J. Catal.*, **290**, 186 (2012).
36. X. Chen, M. Dong, X. Niu, K. Wang, G. Chen, W. Fan, J. Wang and Z. Qin, *Chin. J. Catal.*, **36**, 880 (2015).